Current Photovoltaic Research 12(4) 135-141 (2024)
DOI:https://doi.org/10.21218/CPR.2024.12.4.135
pISSN 2288-3274
eISSN 2508-125X

Photoelectrodeposition of NiMo Catalyst on Cu_2O Photocathodes for Enhanced Solar-to-Hydrogen Energy Conversion

Ji Hoon Choi† · Ji Hye Jeong† · Hak Hyeon Lee · Hyung Koun Cho*

School of Advanced Materials Science and Engineering, Sungkyunkwan University, Suwon, 16419, Korea

Received October 28, 2024; Revised December 5, 2024; Accepted December 10, 2024

ABSTRACT: Photoelectrochemical (PEC) water splitting offers an eco-friendly method to convert solar energy into hydrogen, with recent advancements improving efficiency. However, despite direct hydrogen production on photocathode surfaces, research into high-performance, stable photocathode-specific catalysts remains limited. In this study, we optimized a NiMo hydrogen evolution reaction (HER) catalyst on Cu_2O-based photocathodes using a photoelectrodeposition (PED) method to enhance PEC water-splitting efficiency. Key deposition parameters, including light, current density, applied voltage, and time, were systematically controlled to ensure uniform NiMo catalyst deposition without post-treatments. Under simulated 1-sun illumination, the optimized NiMo catalyst achieved 93% of the performance of conventional Pt catalysts and maintained stable hydrogen production for over 20 hours. Electrochemical analysis confirmed superior PEC performance of the NiMo catalyst, particularly at a fixed current density of −1.5 μA cm^{-2}. This study introduces a noble metal-free catalyst deposition method, advancing solar-to-hydrogen conversion efficiency and long-term PEC device stability.

Key words: Photoelectrochemical cell, NiMo catalyst, Hydrogen evolution reaction, Cu_2O photocathodes

Subscript

PEC : photoelectrochemical
HER : hydrogen evolution reaction
PED : photoelectrodeposition
ETL/HTL : electron/hole transport layer
LSV : linear sweep voltammetry

1. Introduction

Harnessing solar energy for power generation is a crucial strategy to replace fossil fuels, and extensive research has been conducted in this field[1-3]. Solar cells, which are widely used in the market today, generate electrical energy, and recent studies have focused on organic halide perovskites as alternatives to Si-based substrates[4-7]. Among the various solar cell technologies, photoelectrochemical (PEC) cells offer the advantage of coupling light-absorbing semiconductors with electron/hole transport layers (ETL and HTL) for direct water splitting and hydrogen production[8-14]. While using the electricity generated by solar cells for water splitting involves a two-step process with thermal energy losses, PEC cells enable the direct storage of high-purity hydrogen and oxygen from the electrolyte, offering a more efficient solution. However, the simultaneous occurrence of light exposure, applied voltage, and chemical reactions imposes significant damage on semiconductor devices, limiting their performance and stability, leading to low hydrogen production efficiencies. To address these challenges, numerous studies have explored novel materials[15-17], *p*/*n* junctions[18, 19], surface-limited catalysts[20, 21], and doping strategies[22].

In contrast to light-absorbing layers in solar cells, PEC cells require an overpotential greater than 1.6 eV to drive water splitting, making materials with a bandgap of 1.6−2.4 eV highly suitable[23]. Among these, photocathodes used for direct hydrogen production are more prone to instability compared to photo-anodes, making them a key factor in determining the overall efficiency of PEC hydrogen production[18, 20]. Cu_2O photocathodes, composed of earth-abundant elements, possess a 2.1 eV bandgap, enabling efficient use of visible light[18, 20, 24]. Moreover, electro-deposited Cu_2O allows for nanoscale thickness control and crystallinity adjustment through pH modulation, making it an ideal material for large-area PEC devices[25]. However, Cu_2O

†These authors equally contributed to this work.
*Corresponding author: chohk@skku.edu

suffers from rapid photocorrosion when operated without additional processes, necessitating the incorporation of *n*-type AZO/TiO_2 buffer and passivation layers[18, 20]. In most recent studies, Pt catalysts for the hydrogen evolution reaction (HER) are deposited on the ETL surface using e-beam evaporation or photo-/electrochemical methods to drive water splitting[24, 26]. Despite these advances, the hydrogen production photocurrent density remains lower than the theoretical efficiency of light-absorbing layers. While discovering new materials for light-absorbing layers and ETLs is important, the key to improving hydrogen production in PEC cells lies in the deposition of highly active, surface-limited HER catalysts on the reaction sites. Nevertheless, many recent studies continue to rely on precious Pt catalyst for this purpose.

In this study, we addressed the need for a new catalyst that can replace the precious Pt catalyst while maintaining high HER activity and stability. As large-scale PEC devices are the ultimate goal, it is essential to develop catalysts composed of earth-abundant elements that can be deposited on light-absorbing layers without causing damage. Therefore, we selected NiMo as a promising catalyst due to its abundance, high HER activity, and operation stability. For PEC hydrogen production, we successfully deposited a NiMo catalyst on Cu_2O-based photocathodes by optimizing various parameters and applied it to solar H_2 production.

Here, we highlight a significant advancement in the application of earth-abundant materials for PEC hydrogen production, offering an alternative to the traditional reliance on Pt catalysts in previous research. The NiMo catalyst was deposited using an optimized electrodeposition technique, unlike conventional vacuum-based processes that require high vacuum conditions, elevated temperatures, and significant electricity consumption[27]. This electrodeposition approach is compatible with the Cu_2O photocathode surface, effectively addressing dual challenges of cost-efficiency and material stability.

Furthermore, the synergistic interaction between nickel and molybdenum in the catalyst enhances HER kinetics, providing performance comparable to Pt in terms of overpotential and stability under operating conditions[28]. This study not only underscores the potential of NiMo as a practical alternative to Pt but also demonstrates the feasibility of scalable PEC device fabrication using cost-effective and sustainable materials.

2. Experimental Methods

2.1 Device fabrication process

To fabricate the Cu_2O photocathode, indium tin oxide (ITO) substrates were cleaned sequentially in acetone, ethanol, and DI water for 20 minutes each. The Cu_2O was prepared as a double-layer Cu_2O (D-Cu_2O) consisting of Sb-doped Cu_2O (Sb-Cu_2O, 200 nm) and undoped Cu_2O (1.1 μm). Electrodeposition was performed using a three-electrode system with a potentiostat (VersaSTAT4; Princeton Applied Research), employing an Ag/AgCl reference electrode and a Pt mesh counter electrode.

The Sb-doped Cu_2O, serving as the HTL, was fabricated from an electrolyte composed of 0.4 M copper sulfate ($CuSO_4$), 3 M lactic acid ($CH_3CH(OH)CO_2H$), and 3 mM antimony(III) sulfate ($Sb_2(SO_4)_3$) in DI water. The electrolyte's pH was adjusted to 10 using 4 M sodium hydroxide (NaOH), and the temperature was maintained at 60°C. The undoped Cu_2O was electrodeposited using an electrolyte of 0.4 M copper sulfate and 3 M lactic acid dissolved in DI water, with the pH set to 11 and a temperature of 60°C. During electrodeposition, a potential of −0.5 $V_{Ag/AgCl}$ was applied until charges of −0.166 and −0.913 C were reached for Sb-Cu_2O and undoped Cu_2O layers, respectively.

The *n*-type Al-doped ZnO (AZO) buffer layer and TiO_2 passivation layer were both deposited using atomic layer deposition. Diethylzinc (DEZn, $(C_2H_5)_2Zn$) and trimethylaluminum (TMA, $Al_2(CH_3)_6$) were used as precursors for AZO, with H_2O as the oxygen source. The deposition was carried out at 150°C in a nitrogen atmosphere, resulting in a 20 nm film. TiO_2 was deposited using tetrakis(dimethylamino)titanium (TDMAT) as the precursor, with H_2O as the reactant, at a chamber temperature of 100°C in an argon atmosphere, producing a 30 nm layer.

The Pt and NiMo catalysts were both formed by electrodeposition using a three-electrode system with a potentiostat (VersaSTAT4). An Ag/AgCl reference electrode and a Pt mesh counter electrode were used, and galvanostatic deposition was conducted under 1-sun illumination (NiMo catalyst). For Pt deposition, the electrolyte consisted of 1 mM chloroplatinic acid (H_2PtCl_6) dissolved in DI water, with a fixed current density of −8.5 μA cm^{-2}. The NiMo catalyst was deposited from an electrolyte of 1 M nickel(II) sulfamate tetrahydrate ($Ni(SO_3NH_2)_2$), 2 mM sodium molybdate dihydrate ($NaMoO_4$), and 0.5 M boric acid (H_3BO_3) in 100 mL of DI water, using a fixed current density of −1.5 μA cm^{-2}. Detailed electrodeposition, thin film and catalysts fabrication can be found in our previous reports[10, 29].

2.2 Analysis methods

PEC measurements were performed under 100 mW cm^{-2} AM 1.5 G illumination using a three-electrode system (VersaSTAT4). An Ag/AgCl reference electrode and a Pt mesh counter electrode were used, and the potentials were converted to the RHE scale using the Nernst equation. The electrolyte used for PEC measurements, including the incident photon-to-current efficiency (IPCE) evaluation, was composed of 0.5 M Na_2SO_4, 0.1 M KH_2PO_4, and 0.2 M H_3BO_3 dissolved in DI water, with the pH adjusted to 5 using KOH. The samples were analyzed using scanning electron microscopy (SEM) and energy-dispersive X-ray spectroscopy (EDS). Additionally, X-ray photoelectron spectroscopy (XPS; SIGMA PROBE, Thermo Fisher Scientific) was performed for further characterization.

3. Results and Discussion

Fig. 1(a) illustrates the typical structure of a half-cell photocathode. In this configuration, the photocathode creates an internal electric field due to the band bending effect at the interface with the electrolyte. When light is applied, photo-excited electrons are driven towards the electrolyte, where they participate in the HER, while the connected counter electrode facilitates the OER. The HER catalyst on the photocathode must meet the following criteria: (1) high HER activity, (2) uniform deposition, (3) earth-abundant materials, and (4) no damage to the electrode. Fig. 1(b) shows the configuration of the three-electrode system used for PEC measurements with a Cu_2O-based photocathode. This highlights the practical application of the half-cell photocathode structure presented in Fig. 1(a).

As shown in Fig. 1(c), vacuum-based deposition methods, such as e-beam evaporation, have the advantage of uniformly depositing metals and minimizing electrode damage, but they face significant limitations in scalability. Moreover, a major drawback is the lack of preferential catalyst deposition on high surface energy regions that arise from surface defects on the photoelectrode. This non-selective deposition results in reduced stability during PEC water splitting.

To address this issue, we propose a method for selective deposition of a NiMo catalyst on a Cu_2O-based photocathode. By illuminating the photocathode with simulated 1-sun and applying a mild bias, we can electrodeposit NiMo from a precursor solution containing dissolved Ni and Mo. Compared to electrodeposition without light illumination, photoelectrodeposition (PED) facilitates the formation of the NiMo catalyst by providing sufficient photo-excited electrons to the electrode surface even at a lower potential. Additionally, this method occurs primarily on the photocathode surface, overcoming the previous limitations. Furthermore, this approach ensures that the NiMo catalyst is preferentially deposited along the main current pathways within the photocathode, thereby enhancing the operational stability of the device.

Fig. 2(a) presents cyclic voltammetry data showing the significant difference in reactivity when a Cu_2O-based photocathode is immersed in the NiMo electrodeposition electrolyte, with and without 1-sun illumination. This graph not only allows

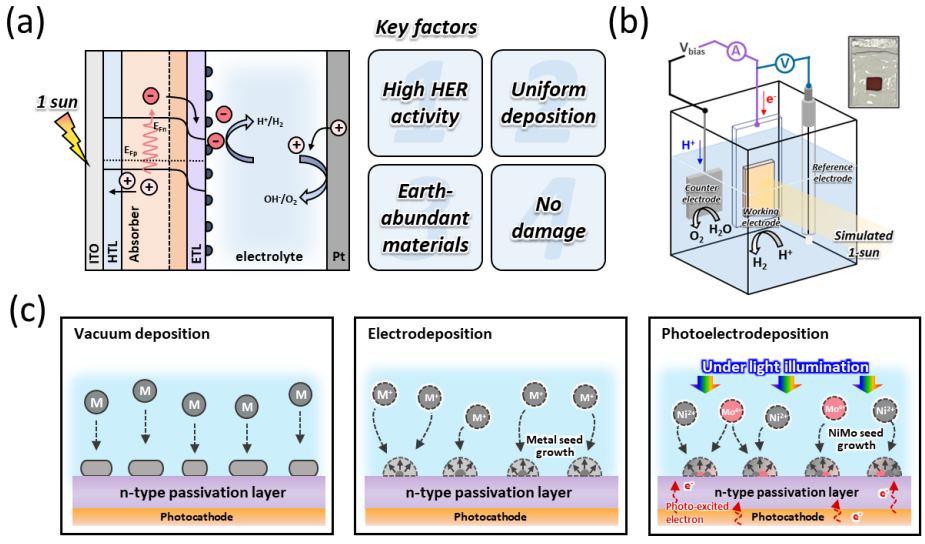

Fig. 1. (a) Structure of the half-cell photocathode and key factors related to HER catalysts, (b) HER reaction of ITO/D-Cu_2O/AZO/TiO_2/NiMo in the measurement cell, (c) comparison of vacuum deposition, electrodeposition, and photoelectrodeposition (PED) methods for catalyst deposition

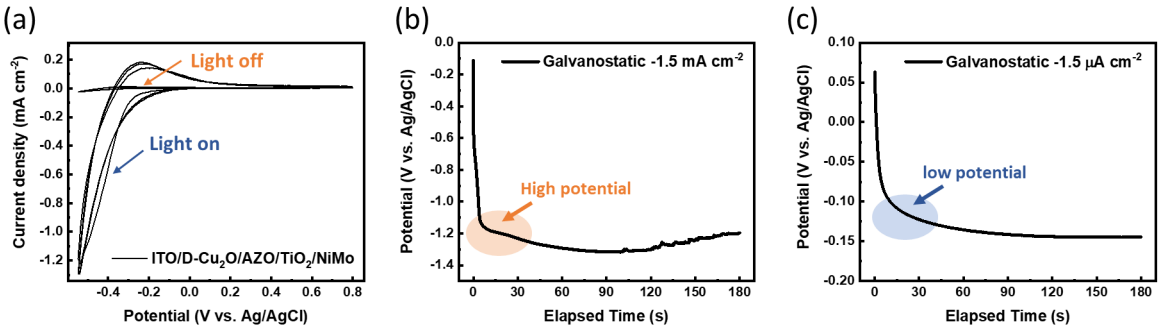

Fig. 2. (a) Cyclic voltammetry data of ITO/D-Cu_2O/AZO/TiO_2/NiMo, and data from galvanostatic deposition at fixed current densities of (b) −1.5 mA cm^{-2} and (c) −1.5 μA cm^{-2}, respectively

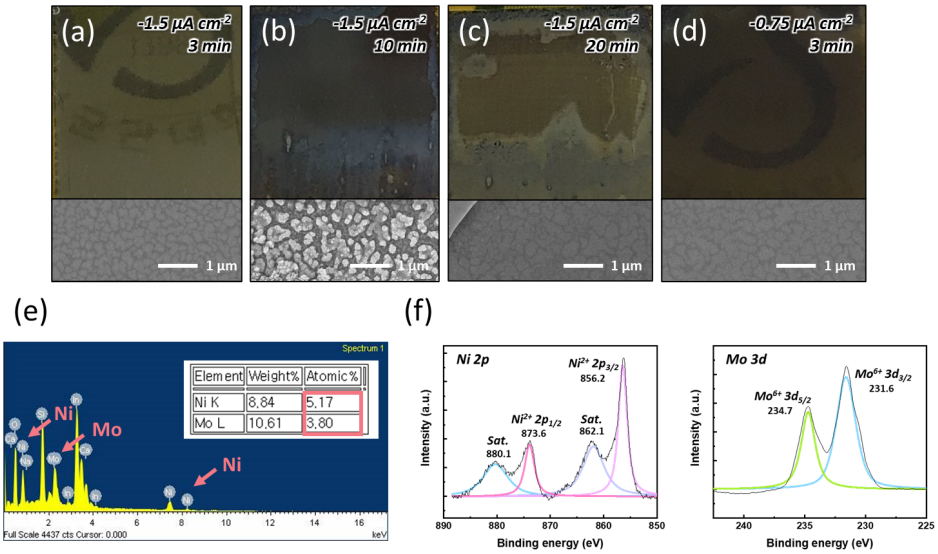

Fig. 3. Photo-images and SEM images of samples deposited at a fixed current density of −1.5 μA cm^{-2} with varying deposition times: (a) 3 minutes, (b) 10 minutes, and (c) 20 minutes. (d) Sample deposited at a fixed current density of −0.75 μA cm^{-2} for 3 minutes. (e) EDS data and (f) XPS data of the sample deposited at −1.5 μA cm^{-2} for 20 minutes

us to identify the potential window where NiMo deposition occurs but also demonstrates that light significantly enhances the catalyst deposition process.

In Figs. 2(b) and (c), we adopted a galvanostatic method to carry out PED under 1-sun for 3 minutes at two fixed photocurrent densities: a relatively high current density of −1.5 mA cm^{-2} and a low current density of −1.5 μA cm^{-2}. At high constant current values, the applied voltage to the device increases rapidly and is maintained for 3 minutes. This voltage range is sufficiently high to cause damage to the Cu_2O photocathode.

In contrast, under the low-current density condition of −1.5 μA cm^{-2}, the galvanostatic conditions maintain a stable and low applied voltage between −120 and −130 $mV_{Ag/AgCl}$, as shown in the graph in Fig. 2(c). This stable, noise-free deposition ensures that NiMo is deposited without causing damage to the photocathode.

Figs. 3(a-c) show the changes in surface morphology when NiMo is electrodeposited for different durations at a constant current of −1.5 μA cm^{-2}. To compare these changes, we performed the deposition for 3, 10, and 20 minutes, capturing surface SEM images along with photographs of the actual 1 cm × 1 cm samples. After 3 minutes at −1.5 μA cm^{-2}, we observed a uniform and thin NiMo catalyst layer deposited on the ITO. However, after 10 minutes, the surface began to exhibit increased roughness and non-uniformity. When the deposition was extended to 20 minutes, the catalyst thickness became inconsistent, and partial delamination of NiMo was observed.

Additionally, as shown in Fig. 3(d), when a lower current of −0.75 μA cm^{-2} was applied, the surface appeared thicker compared to the deposition at −1.5 μA cm^{-2}, and slight delamination was visible at the upper portion of the sample. This indicates that, even at lower currents, non-optimized conditions

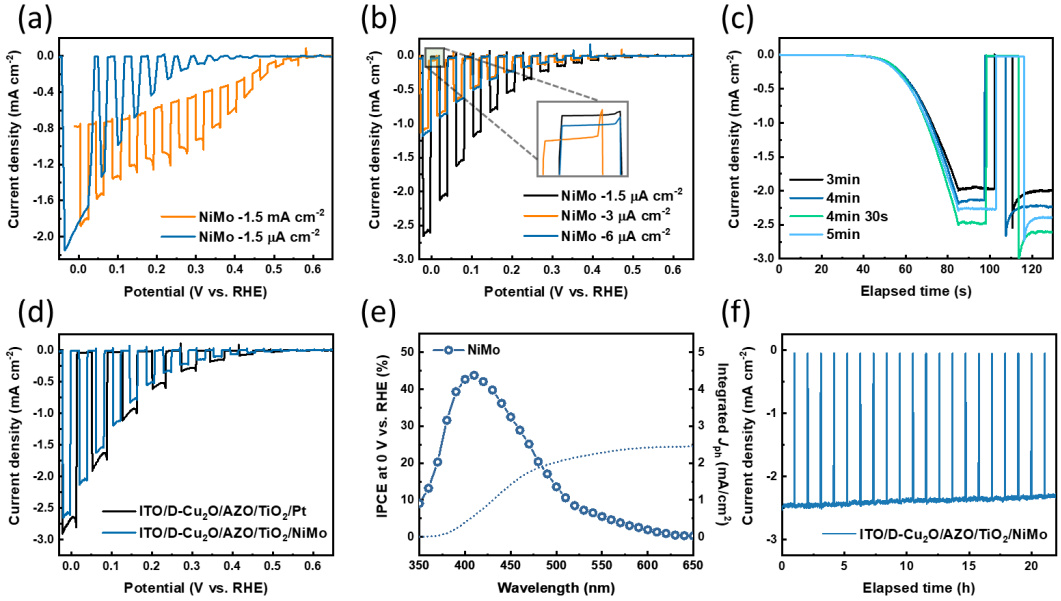

Fig. 4. (a) LSV data measured at fixed currents of −1.5 mA cm^{-2} and −1.5 μA cm^{-2}. (b) LSV data measured at fixed currents of −1.5, −3, and −6 μA cm^{-2}. (c) Combined LSV and CA graph measured at a fixed current of −1.5 μA cm^{-2}. (d) LSV graph comparing the PEC performance of NiMo deposited at −1.5 μA cm^{-2} with that of conventional Pt catalysts. (e) IPCE and integrated photocurrent density of the NiMo catalyst sample deposited at −1.5 μA cm^{-2}. (f) Long-term stability test of the photocathode using NiMo catalysts

can lead to uneven NiMo deposition.

Further analysis, presented in Figs. 3(e) and 3(f), involves EDS measurements to verify the successful deposition of NiMo and XPS measurements for detailed surface characterization. The sample used for this analysis was deposited at −1.5 μA cm^{-2} for 20 minutes on an ITO electrode. According to the EDS analysis, the atomic percentages of Ni and Mo were found to be 5.17% and 3.80%, respectively, confirming the successful deposition of the catalyst. While the Ni:Mo atomic ratio (approximately 1.36:1) is slightly lower than the reported optimal ratio for HER (1.86:1), it is still within a comparable range, suggesting potential for further enhancement of catalytic performance through additional optimization[30]. The XPS analysis provides additional evidence for the successful formation of the NiMo catalyst by identifying characteristic peaks corresponding to Ni and Mo elements on the surface. Ni primarily facilitates hydrogen adsorption, while Mo promotes hydrogen desorption, effectively enhancing HER activity through their complementary catalytic roles[30, 31].

Based on the above results, we compared the PEC water-splitting performance under various conditions to optimize the NiMo catalyst on the surface. ITO/D-Cu_2O/AZO/TiO_2 photo cathodes were used in the PED method. Fig. 4(a) presents linear sweep voltammetry (LSV) curves measured by chopping under simulated 1-sun, after performing PED of NiMo at fixed currents of −1.5 μA cm^{-2} and −1.5 mA cm^{-2} for 3 minutes. As seen in Fig. 2(a), the fixed current of −1.5 mA cm^{-2} induces a high applied voltage of −1.2 $V_{Ag/AgCl}$, which damages the Cu_2O, leading to significant dark current at potentials below 0.5 V_{RHE}. This indicates that the device is not properly on/off during PEC operation, suggesting that the generated photocurrent is directed toward side reactions rather than the HER.

As shown in Fig. 4(b), PEC measurements were also performed at fixed currents of −3 and −6 μA cm^{-2}, and the photocurrent density significantly decreased compared to −1.5 μA cm^{-2} condition. Additionally, the off current of the sample deposited at −1.5 μA cm^{-2} sample was closest to zero current, indicating that the Cu_2O photocathode operated effectively under illumination without other side reactions. Fig. 4(c) shows that after selecting −1.5 μA cm^{-2} as the optimal fixed current, LSV measurements were conducted with varying PED deposition times. The sample deposited for 4 minutes, and 30 seconds exhibited the best performance, while performance declined with 5 minutes.

Additionally, in Fig. 4(d), we compared the PEC performance of the NiMo catalyst, deposited at −1.5 μA cm^{-2} for 4 minutes and 30 seconds, with that of Pt. Although the LSV curve of the Pt-deposited sample showed higher performance, the optimized NiMo catalyst achieved approximately 93% of the performance of Pt. Fig. 4(e) presents the IPCE analysis of the Cu_2O-based

photocathode incorporating the NiMo catalyst, revealing a peak efficiency of approximately 45% within the 400–430 nm wavelength range, signifying effective photon-to-electron conversion in the visible spectrum. The integrated photocurrent density reached approximately 2.5 mA cm^{-2}, highlighting the role of the NiMo catalyst in enhancing the photoelectrochemical performance. In Fig. 4(f), the long-term operational stability of the NiMo catalyst was evaluated at 0 V_{RHE}. The catalyst demonstrated stable PEC HER operation for 20 hours, maintaining 95% of its initial photocurrent density.

4. Conclusions

In this study, we optimized the deposition of a NiMo HER catalyst on Cu_2O-based photocathodes using the photoelectrodeposition (PED) method and evaluated its water-splitting hydrogen production performance. The optimization process involved controlling factors such as light intensity, current density, applied voltage, and deposition time. The NiMo catalyst was deposited via PED without the need for additional post-treatment or activation steps. Under 1-sun illumination, the HER performance of the NiMo catalyst reached approximately 93% of that achieved by Pt catalysts deposited using the same PED method, while maintaining stable operation over 20 hours. These results demonstrate the successful synthesis of a highly efficient PEC water-splitting catalyst using earth-abundant elements. By proposing a novel deposition method for NiMo surface-limited catalysts, which has been less emphasized in previous PEC energy conversion research, this study provides valuable insights for future developments in the field.

Acknowledgments

This work was supported by the National Research Foundation of Korea (NRF) grant funded by the Korea government (MSIT) (2021R1A2C3011870).

References

1. P. K. Nayak, S. Mahesh, H. J. Snaith, D. Cahen, Photovoltaic solar cell technologies: analysing the state of the art. Nat. Rev. Mater. 4, 269-285 (2019).
2. T. Hisatomi, J. Kubota, K. Domen, Recent advances in semiconductors for photocatalytic and photoelectrochemical water splitting. Chem. Soc. Rev. 43, 7520-7535 (2014).
3. H. S. Jung, N. G. Park, Perovskite Solar Cells: From Materials to Devices. Small. 11(1), 10-25 (2015).
4. J. Y. Kim, J. W. Lee, H. S. Jung, H. J. Shin, N. G. Park, High-Efficiency perovskite solar cells. Chem. Rev. 120(15), 7867-7918 (2020).
5. H. J. Hong, S. M. Lee, J. M. Im, J. H. Noh, Study for improved photocurrent via high concentrated tin-lead perovskite precursor solution. Current Photovoltaic Research. 11(3), 96-102 (2023).
6. H. Y. Lee, S. B. Hong, D. H. Kim, Study on auger recombination control using barrier SiO_2 in high-quality polysilicon/tunneling oxide based emitter formation. Current Photovoltaic Research. 12(2), 31-36 (2024).
7. H. J. Seok, D. K. Lee, H. K. Kim, Multicoated flexible indium tin oxide electrodes fabricated using magnetron sputtering and arc plasma ion plating for flexible perovskite solar cells. ACS Appl. Mater. Interfaces. 16(36), 47961-47972 (2024).
8. Y. Yang, S. Niu, D. Han, T. Liu, G. Wang, Progress in developing metal oxide nanomaterials for photoelectrochemical water splitting. Adv. Energy Mater. 7, 1700555 (2017).
9. S. Chen, T. Liu, Z. Zheng, M. Ishaq, G. Ling, P. Fan, T. Chen, J. Tang, Recent progress and perspectives on Sb_2Se_3-based photocathodes for solar hydrogen production via photoelectrochemical water splitting. J. Energy Chem. 67, 508-523 (2022).
10. J. H. Choi, D. S. Kim, Y. B. Kim, S. H. Jung, S. Sarker, N. G. Deshpande, H. H. Lee, H. W. Suh, H. K. Cho, Bundle-type columnar Cu_2O photoabsorbers with vertical grain boundaries fabricated using instant strike-processed metallic seeds and their enhanced photoelectrochemical efficiency. ACS Sustainable Chem. Eng. 9(18), 6390-6399 (2021).
11. H. J. Seok, S. H. Kim, K. M. Yeom, J. H. Noh, H. K. Kim, Cost-effective transparent n-doped tin oxide electrodes with excellent thermal and chemical stabilities enabling stable perovskite photovoltaics based on tin oxide electron transport layer. Adv. Energy Mater. 14, 2303859 (2024).
12. J. W. Yang, S. G. Ji, C. S. Jeong, J. H. Kim, H. R. Kwon, T. H. Lee, S. A. Lee, W. S. Cheon, S. J. Lee, H. S. Lee, M. S. Kwon, J. H. Moon, J. Y. Kim, H. W. Jang, High-efficiency unbiased water splitting with photoanodes harnessing polycarbazole hole transport layers. Energy Environ. Sci. 17, 2541 (2024).
13. H. S. Han, W. S. Park, A. Sivanantham, S. W. Hwang, S. Surendran, U. Sim, I. S. Cho, Facile fabrication of nanotubular heterostructure for enhanced photoelectrochemical performance. Ceram. Int. 47(3), 3972-3977 (2021).
14. H. S. Han, W. S. Park, S. W. Hwang, H. K. Kim, Y. L. Sim, S. Surendran, U. Sim, I. S. Cho, (020)-Textured tungsten trioxide nanostructure with enhanced photoelectrochemical activity. J. Catal. 389, 328-336 (2020).
15. W. S. Yang, S. M. Lee, H. C. Kwon, J. Tan, H. S. Lee, J. M. Park, Y. J. Oh, H. Y. Choi, J. H. Moon, Time-resolved observations of photo-generated charge-carrier dynamics in Sb_2Se_3 photocathodes for photoelectrochemical water splitting.

ACS Nano. 12(11), 11088-1109 (2018).

16. G. Liang, Z. Li, M. Ishaq, Z. Zheng, Z. Su, H. Ma, X. Zhang, P. Fan, S. Chen, Charge separation enhancement enables record photocurrent density in $Cu_2ZnSn(S,Se)_4$ photocathodes for efficient solar hydrogen production. Adv. Energy Mater. 13, 2300215 (2023).
17. R. Rhee, T. G. Kim, G. Y. Jang, G. M. Bae, J. H. Lee, S. J. Lee, S. S. Kim, S. W. Jeon, J. H. Park, Unassisted overall water splitting with a solar-to-hydrogen efficiency of over 10% by coupled lead halide perovskite photoelectrodes. Carbon Energy. 5, e232 (2023).
18. A. Paracchino, V. Laporte, K. Sivula, M. Grätzel, E. Thimsen, Highly active oxide photocathode for photoelectrochemical water reduction. Nature Mater. 10, 456-461 (2011).
19. G. K. Seo, B. N. Kim, S. W. Hwang, S. S. Shin, I. S. Cho, High-performance bulky crystalline copper bismuthate photocathode for enhanced solar water splitting. Nano Energy. 80, 105568 (2021).
20. J. H. Choi, H. H. Lee, S. H. Jeon, S. Sarker, D. S. Kim, E. A. Stach, H. K. Cho, Photoilluminated redox-processed rh_2p nanoparticles on photocathodes for stable hydrogen production in acidic environments. ACS Appl. Mater. Interfaces. 16(17), 21953-21964 (2024).
21. M. Xia, L. Pan, Y. Liu, J. Gao, J. Li, M. Mensi, K. Sivula, S. M. Zakeeruddin, D. Ren, M. Grätzel, Efficient Cu_2O photocathodes for aqueous photoelectrochemical CO_2 reduction to formate and syngas. J. Am. Chem. Soc. 145(51), 27939-27949 (2023).
22. M. Zhang, J. Wang, H. Xue, J. Zhang, S. Peng, X. Han, Y. Deng, W. Hu, Acceptor-doping accelerated charge separation in Cu_2O photocathode for photoelectrochemical water splitting: Theoretical and experimental studies. Angew. Chem. 132, 18621-18625 (2020).
23. J. H. Kim, D. Hansora, P. Sharma, J. W. J. S. Lee, Toward practical solar hydrogen production–an artificial photosynthetic leaf-to-farm challenge, Chem. Soc. Rev. 48, 1908-1971 (2019).
24. L. Pan, J. H. Kim, M. T. Mayer, M. K. Son, A. Ummadisingu, J. S. Lee, A. Hagfeldt, J. Luo, M. Grätzel, Boosting the performance of Cu_2O photocathodes for unassisted solar water splitting devices. Nat. Catal. 1, 412-420 (2018).
25. A. Paracchino, J. C. Brauer, J. E. Moser, E. Thimsen, M. Grätzel, Synthesis and characterization of high-photoactivity electrodeposited Cu_2O solar absorber by photoelectrochemistry and ultrafast spectroscopy. J. Phys. Chem. C. 116, 7341-7350 (2012).
26. J. H. Choi, D. S. Kim, S. Sarker, H. H. Lee, H. W. Suh, S. H. Jung, K. W. Lee, H. S. Lee, H. K. Cho, Atomic-scale platinum deposition on photocathodes by multiple redox cycles under illumination for enhanced solar-to-hydrogen energy conversion. J. Power Sources. 533, 231410 (2022).
27. S. A. Lee, J. W. Yang, S. K. Choi, H. W. Jang, Nanoscale electrodeposition: Dimension control and 3D conformality. Exploration. 1(3), 20210012 (2021).
28. J. R. McKone, E. L. Warren, M. J. Bierman, S. W. Boettcher, B. S. Brunschwig, N. S. Lewis, H. B. Gray, Evaluation of Pt, Ni, and Ni–Mo electrocatalysts for hydrogen evolution on crystalline Si electrodes. Energy Environ. Sci. 4, 3573 (2011).
29. J. H. Choi, H. J. Seok, D. C. Sung, D. S. Kim, H. H. Lee, S. Hong, H. K. Kim, H. K. Cho, Electrodeposited copper oxides with a suppressed interfacial amorphous phase using mixed-crystalline ITO and their enhanced photoelectrochemical performances. J. Energy Chem. 82, 277-286 (2023).
30. D. Neumüller, L. D. Rafailović, I. A. Pašti, T. Griesser, C. Gammer, J. Eckert, Revealing the role of mo leaching in the structural transformation of NiMo thin film catalysts upon hydrogen evolution reaction. Small. 20, 2402200 (2024).
31. A. Nairan, P. Zou, C. Liang, J. Liu, D. Wu, P. Liu, C. Yang, NiMo solid solution nanowire array electrodes for highly efficient hydrogen evolution reaction. Adv. Funct. Mater. 29, 1903747 (2019).